

Vibrational relaxation of trapped molecules

R. C. Forrey, V. Kharchenko, N. Balakrishnan, and A. Dalgarno

*Institute for Theoretical Atomic and Molecular Physics, Harvard-Smithsonian Center for Astrophysics,
60 Garden Street, Cambridge, Massachusetts 02138*

(Received 20 October 1998)

Vibrational relaxation of trapped molecules due to collisions with cold atoms is investigated using the results of quantum-mechanical scattering calculations. Trap loss is analyzed using an exactly solvable kinetic model that includes direct collisional quenching and an indirect process of vibrational predissociation. At low atom density, the relaxation is due primarily to collisional quenching. At high atom density, the relaxation involves additional time scales due to the formation and decay of van der Waals complexes. It is shown that the most weakly bound state of the van der Waals complex for a given diatomic vibrational level controls the relaxation at all atom densities. Possible experiments using trapped molecules are discussed. [S1050-2947(99)05303-2]

PACS number(s): 32.80.Pj

I. INTRODUCTION

Experimental efforts to trap molecules [1–5] have motivated recent investigations of collisional quenching [6,7] and vibrational predissociation [8,9] of diatomic systems. Trapped molecules provide a unique opportunity to study the threshold behavior of collisions between atoms and molecules [6]. Measurement of Feshbach resonances in scattering cross sections would give valuable information about the atom-molecule potential energy surface [9].

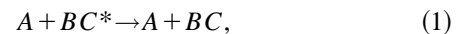
Predissociation may play an important role in the relaxation of vibrationally excited molecules when the density of surrounding atoms is high and the time scale for establishing equilibrium of van der Waals molecules is short compared to other relaxation processes [10]. Therefore, it may be possible to use the relaxation of vibrationally excited trapped molecules as a means for obtaining the Feshbach resonance parameters. In the present work, we investigate this possibility for trapped diatomic molecules by including predissociation in the kinetic theory of vibrational relaxation. Using calculated quenching rates and predissociation lifetimes for a realistic system, we make estimates of the relaxation time for vibrationally excited trapped molecules as a function of atom density. The role of the most weakly bound state of the van der Waals complex is investigated for both the low and high density limits. It is shown that a single measurement of vibrational relaxation of trapped molecules performed at high atom density would uniquely determine the binding energy and predissociation lifetime of the van der Waals complex, the collisional rate of formation of the complex, and the zero-temperature quenching rate of the excited diatom.

The paper is organized as follows. In Sec. II we present the kinetic model for trapped molecules. Section III reviews the exact close-coupling formulation for computing cross sections and lifetimes. In Sec. IV, we use perturbation theory to analyze the relationship between the binding energy of a weakly bound complex and its predissociation decay rate. Effective range theory is used in Sec. V to provide estimates of predissociation lifetimes for the most weakly bound levels. Section VI discusses the detailed balance between the collisional rate of van der Waals formation and decay. In Sec. VII we give some numerical results for the two isotopes

of helium interacting with vibrationally excited H_2 . Atomic units are assumed throughout the paper.

II. KINETIC MODEL

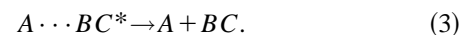
Relaxation of vibrationally excited trapped diatomic molecules may occur through the direct collisional quenching process



where A is a trapped atom, BC^* is the initial excited diatom with vibrational quantum number v and rotational quantum number j , and BC is any final state diatom with quantum numbers v' and j' different from v and j . The internal energy of the initially excited diatom is transferred to translational energy with rate coefficient R_{vj} . The vibrational energy spacing of the diatom is typically much larger than the depths of experimental traps and we may assume that quenched molecules are immediately removed from the trap. A two-step mechanism may also remove molecules from the trap. In the first step, the molecules form a van der Waals complex $A \cdots BC^*$,



through collision with atoms A . If the binding energy of the complex is less than the trap depth, then the van der Waals molecule may remain within the trap. The complex may then decay after a finite lifetime τ_{vj} through the process of vibrational predissociation,



In the absence of radiative transitions, the collisional loss may be described by the kinetic equations

$$\begin{aligned} \frac{d}{dt}[BC^*]_t + (R_{vj}[A] + k_f[A]^2)[BC^*]_t \\ = k_b[A][A \cdots BC^*]_t, \end{aligned} \quad (4)$$

$$\begin{aligned} \frac{d}{dt}[A \cdots BC^*]_t + (\tau_{vj}^{-1} + k_b[A])[A \cdots BC^*]_t \\ = k_f[A]^2[BC^*]_t, \end{aligned} \quad (5)$$

where $[BC^*]_t$ and $[A \cdots BC^*]_t$ are the respective densities of BC^* and $A \cdots BC^*$ at time t after an initial source of BC^* has been turned off. The density of cold atoms $[A]$ is assumed to be constant. The rate coefficients for the forward and backward reaction (2) are given by k_f and k_b , respectively. Equations (4) and (5) may be combined into a single second-order differential equation,

$$\begin{aligned} \frac{d^2}{dt^2}[BC^*]_t + \{\tau_{vj}^{-1} + (R_{vj} + k_b)[A] + k_f[A]^2\} \frac{d}{dt}[BC^*]_t \\ + \{\tau_{vj}^{-1}R_{vj}[A] + (k_bR_{vj} + \tau_{vj}^{-1}k_f)[A]^2\}[BC^*]_t \\ = 0 \end{aligned} \quad (6)$$

with the solution

$$[BC^*]_t = [BC^*]_0(c_1 e^{-\lambda_1 t} + c_2 e^{-\lambda_2 t}), \quad (7)$$

where

$$\lambda_1 = \frac{1}{2}(\alpha + \beta), \quad (8)$$

$$\lambda_2 = \frac{1}{2}(\alpha - \beta), \quad (9)$$

$$\alpha = \tau_{vj}^{-1} + (R_{vj} + k_b)[A] + k_f[A]^2, \quad (10)$$

$$\beta = \sqrt{[\tau_{vj}^{-1} + (k_b - R_{vj})[A] - k_f[A]^2]^2 + 4k_f k_b [A]^3}, \quad (11)$$

$$c_1 = \left(\frac{R_{vj}[A] + k_f[A]^2 - \lambda_2 - k_b[A] \frac{[A \cdots BC^*]_0}{[BC^*]_0}}{\lambda_1 - \lambda_2} \right), \quad (12)$$

and

$$c_2 = \left(\frac{\lambda_1 - R_{vj}[A] - k_f[A]^2 + k_b[A] \frac{[A \cdots BC^*]_0}{[BC^*]_0}}{\lambda_1 - \lambda_2} \right). \quad (13)$$

If the time scale for establishing equilibrium of van der Waals molecules is short compared to other relaxation processes, then we may assume a steady-state solution to Eq. (5) during the time that the trapped molecules are being produced. The initial condition needed by Eqs. (12) and (13) is then given by

$$\frac{[A \cdots BC^*]_0}{[BC^*]_0} = \frac{k_f[A]^2}{\tau_{vj}^{-1} + k_b[A]}. \quad (14)$$

If we define

$$\epsilon = \frac{k_f k_b [A]^3}{|\tau_{vj}^{-1} + (k_b - R_{vj})[A] - k_f[A]^2|^2} \quad (15)$$

and

$$\gamma = \frac{R_{vj}[A] + k_f[A]^2}{\tau_{vj}^{-1} + k_b[A]} \quad (16)$$

and assume that $\epsilon \ll 1$, then the relaxation path is controlled by the value of γ . For $\gamma > 1$ or $\gamma < 1$, the time scales are given by

$$\lambda_1 = (1 - \gamma^{-1}\epsilon)(R_{vj}[A] + k_f[A]^2), \quad (17)$$

$$\lambda_2 = (1 - \gamma\epsilon)(\tau_{vj}^{-1} + k_b[A]) \quad (18)$$

with $c_1 = 1 - \gamma\epsilon$ and $c_2 = \gamma\epsilon$. For $\gamma = 1$, the assumption $\epsilon \ll 1$ breaks down and the formulas (8)–(13) must be used. In the low density limit, $\gamma < 1$ and the relaxation is controlled by the quenching time scale $\lambda_1 = R_{vj}[A]$. In the high density limit, $\gamma > 1$ and the relaxation is controlled by the predissociation time scale $\lambda_2 = \tau_{vj}^{-1}$.

The above discussion may be generalized to include van der Waals interactions that support more than one bound state. For example, if we consider a two-level system labeled $A \cdots BC_1^*$ and $A \cdots BC_2^*$, then the kinetic equations (4) and (5) must be replaced by

$$\begin{aligned} \frac{d}{dt}[BC^*]_t + (R_{vj}[A] + k_{f,1}[A]^2 + k_{f,2}[A]^2)[BC^*]_t \\ = k_{b,1}[A][A \cdots BC_1^*]_t + k_{b,2}[A][A \cdots BC_2^*]_t, \end{aligned} \quad (19)$$

$$\begin{aligned} \frac{d}{dt}[A \cdots BC_1^*]_t + (\tau_{vj,1}^{-1} + k_{b,1}[A])[A \cdots BC_1^*]_t \\ = k_{f,1}[A]^2[BC^*]_t, \end{aligned} \quad (20)$$

$$\begin{aligned} \frac{d}{dt}[A \cdots BC_2^*]_t + (\tau_{vj,2}^{-1} + k_{b,2}[A])[A \cdots BC_2^*]_t \\ = k_{f,2}[A]^2[BC^*]_t, \end{aligned} \quad (21)$$

resulting in a third-order differential equation. In Eqs. (19)–(21) we have assumed that inelastic atom-complex collisions are negligible. The solution to Eqs. (19)–(21) may be written

$$[BC^*]_t = [BC^*]_0(c_1 e^{-\lambda_1 t} + c_2 e^{-\lambda_2 t} + c_3 e^{-\lambda_3 t}), \quad (22)$$

where

$$\lambda_1 = \tau_{vj,1}^{-1}, \quad (23)$$

$$\lambda_2 = \tau_{vj,2}^{-1}, \quad (24)$$

$$\lambda_3 = R_{vj}[A] + k_{f,1}[A]^2 + k_{f,2}[A]^2 \quad (25)$$

in the high density limit. The above discussion is similar to the usual master equation analysis where the time scales are determined by the eigenvalues of a rate matrix. In the present case, however, we see that at high densities the important time scales are related directly to the predissociation life-

times and the relaxation time is given by the quasibound level with the longest lifetime.

III. CLOSE-COUPLING EQUATIONS

The kinetic model described above depends on input parameters that may be computed using an exact quantum-mechanical close-coupling formulation. Therefore, we provide a brief review of the close-coupling procedure used in the present work. The atom-diatom Hamiltonian in the center-of-mass frame is given by

$$H = -\frac{1}{2m} \nabla_r^2 - \frac{1}{2\mu} \nabla_R^2 + v(r) + V_I(r, R, \theta), \quad (26)$$

where r is the distance between atoms B and C of the diatom, R is the distance between atom A and the center of mass of the diatom, θ is the angle between r and R , m is the reduced mass of the diatom, and μ is the reduced mass of the atom with respect to the diatom. The diatomic Schrödinger equation

$$\left[\frac{1}{2m} \frac{d^2}{dr^2} - \frac{j(j+1)}{2mr^2} - v(r) + \epsilon_{vj} \right] \chi_{vj}(r) = 0 \quad (27)$$

is solved by expanding the rovibrational wave function $\chi_{vj}(r)$ in a Sturmian basis set. The full wave function is expanded in a set of channel functions [$n \equiv (vjl)$],

$$\Psi^{JM}(\vec{R}, \vec{r}) = \frac{1}{R} \sum_n C_n(R) \phi_n(\hat{R}, \vec{r}), \quad (28)$$

$$\begin{aligned} \phi_n(\hat{R}, \vec{r}) &= \frac{1}{r} \chi_{vj}(r) \\ &\times \sum_{m_j} \sum_{m_l} (j l J | m_j, M - m_l) Y_{m_j}^j(\hat{r}) Y_{m_l}^l(\hat{R}), \end{aligned} \quad (29)$$

where l is the orbital angular momentum of the atom with respect to the diatom, J is the total angular momentum, M is the projection of J onto the space-fixed z axis, and $(j l J | m_j, M - m_l)$ denotes a Clebsch-Gordon coefficient. Operating the Hamiltonian (26) on the channel functions (28) leads to a set of coupled equations

$$\begin{aligned} &\left[\frac{d^2}{dR^2} - \frac{l_m(l_m+1)}{R^2} + 2\mu E_m \right] C_m(R) \\ &= \sum_n C_n(R) \langle \phi_m | V_I | \phi_n \rangle, \end{aligned} \quad (30)$$

where E_m is the translational energy and l_m is the orbital angular momentum in the m th channel. The close-coupling equations (30) are solved using the general inelastic scattering program MOLSCAT [11]. The cross sections and rate coefficients are given by [12]

$$\begin{aligned} \sigma_{v,j \rightarrow v',j'} &= \frac{\pi}{2\mu E_{vj}(2j+1)} \sum_{J=0}^{\infty} (2J+1) \\ &\times \sum_{l=|J-j|}^{|J+j|} \sum_{l'=|J-j'|}^{|J+j'|} |\delta_{jj'} \delta_{ll'} \delta_{vv'} - S_{jj',ll',vv'}^J|^2, \end{aligned} \quad (31)$$

$$\begin{aligned} R_{v,j \rightarrow v',j'}(T) &= (8k_B T / \pi \mu)^{1/2} \frac{1}{(k_B T)^2} \\ &\times \int_0^{\infty} \sigma_{v,j \rightarrow v',j'}(E_{vj}) \\ &\times \exp(-E_{vj}/k_B T) E_{vj} dE_{vj}, \end{aligned} \quad (32)$$

where T is the temperature and k_B is the Boltzmann constant. The total quenching rate coefficients R_{vj} needed in the kinetic model of Sec. II are given by

$$R_{vj}(T) = \sum_{v',j'} R_{v,j \rightarrow v',j'}(T). \quad (33)$$

To obtain the predissociation lifetimes, the close-coupling equations are solved for energies below threshold, the S matrix is diagonalized, and the eigenphase sum is differentiated with respect to energy to obtain numerically exact resonance widths. The predissociation lifetime is then given by $\tau_{vj,n} = 1/\Gamma_{vj,n}$, where n is the quantum number of the bound state of the van der Waals complex.

IV. PERTURBATION THEORY

Because the kinetic model presented above shows that the relaxation rate depends most strongly on the quasibound level with the longest predissociation lifetime, it is useful to examine the relationship between decay rate and binding energy for a weakly bound complex. We assume that the binding energy I of the van der Waals complex $A \cdots BC^*$ is small, but well defined, i.e., $\Gamma_i \ll I$. The predissociation rate may then be calculated using perturbation theory. The wave functions in zero-order approximation are calculated by neglecting nondiagonal matrix elements V_{if} , and the decay process is calculated using the standard rule

$$\Gamma_i = \sum_f \Gamma_{i,f} = 2\pi \sum_f g(f) \left| \int \chi_i^0(R) V_{if}(R) \chi_f^0(R) dR \right|^2, \quad (34)$$

where $\chi_{i,f}^0(R) = R \varphi_{i,f}^0(R)$ are the unperturbed radial functions and $g(f)$ is the degree of degeneracy of the final state. For a spherically symmetric initial state $J=0$, $l=0$, and $j=0$, the degeneracy of the final states is given by $g(f) = (2l'+1)$. If the momentum transfer is large, then the final continuum wave function will have many oscillations in the region of overlap, and the decay width will be small. Therefore, the largest partial widths are generally found for values of l' that minimize the amount of transferred momentum [13].

We now derive an asymptotic formula for the predissociation decay rate (34). The initial bound state wave function $\chi_i^0(R)$ may be calculated from the equation

$$\frac{d^2\chi_i^0(R)}{dR^2} - [\kappa^2 + 2mV_{ii}(R)]\chi_i^0(R) = 0, \quad (35)$$

where $\kappa^2 = 2mI$. The binding energy I is an arbitrary small value satisfying the condition of a weakly bound state: $I \ll \max\{|V_{ii}(R)|\}$ for a long-range potential or $\kappa^2 R_0^2 \ll 1$ for a short-range potential of radius R_0 . The strength ξ of the binding potential V_{ii} should be enough to support at least one bound state:

$$\xi = 2m \int_0^\infty V_{ii}(R) R dR \geq 1. \quad (36)$$

In the external area $R > R_0$ of a potential well, where the binding energy is larger than the potential $I = \kappa^2/2m \gg |V_{ii}|$, the potential energy may be neglected in the Schrödinger equation. The function $\chi_i^{(0)}(R)$ may then be approximated by

$$\chi_i^{(0)}(R) \approx \begin{cases} \chi_{>}(R) = N(I) e^{-\kappa R}, & R > R_0 \\ \chi_{<}(R) = N(I) \psi_0(R), & R < R_0, \end{cases} \quad (37)$$

where $N(I)$ is a normalization coefficient. The leading term of the internal solution $\chi_{<}(R)$ may be obtained by solving the Schrödinger equation at zero energy,

$$\frac{d^2\psi_0(R)}{dR^2} - 2mV_{ii}(R)\psi_0(R) = 0, \quad (38)$$

and matching to the external solution $\chi_{>}(R)$ in the boundary area $R \sim R_0$:

$$\chi_i^0(R_0) = N(I) e^{-\kappa R_0}, \quad \frac{d}{dR} \ln[\chi_i^0(R)]_{R=R_0} = -\kappa. \quad (39)$$

For weakly bound states, $\kappa R_0 \ll 1$, the boundary conditions for the internal solution $\psi_0(R)$ may be written as energy independent conditions

$$\psi_0(R_0) = 1; \quad \left. \frac{d\psi_0(R)}{dR} \right|_{R=R_0} = -\kappa \approx 0. \quad (40)$$

The internal part of solution $\chi_{<}(R)$ depends on the binding energy via the normalization factor $N(I)$, which may be calculated as follows:

$$\begin{aligned} \int |\chi_i^0|^2 dR &= \int_0^{R_0} |\chi_{<}(R)|^2 dR + \int_{R_0}^\infty |\chi_{>}(R)|^2 dR \\ &= N^2(I) \left(\text{const } R_0 + \frac{1}{2\kappa} \right) = 1. \end{aligned} \quad (41)$$

Because the binding energy I is small, the normalization is given by

$$N(I) = \sqrt{2\kappa} = (8mI)^{1/4}. \quad (42)$$

Accurate evaluation of the rate of predissociation may be done numerically with the exact radial wave functions and nonadiabatic matrix elements $V_{if}(R)$ using Eq. (34). Since the matrix elements $V_{if}(R)$ decrease at large distances faster than all other functions in Eq. (34), the effective integration area is restricted to distances $R < R_0$. Therefore, the predissociation rate is given asymptotically by

$$\Gamma_i = 4(2mI)^{1/2} \sum_f g(f) \left| \int \psi_0(R) V_{if}(R) \chi_f^0(R) dR \right|^2. \quad (43)$$

Since all terms of the sum in Eq. (43) are independent of binding energy, the decay width varies as $I^{1/2}$ for small I . In the Appendix, we demonstrate the validity of the general asymptotic formula (43) for the special case of the Morse potential.

V. EFFECTIVE RANGE THEORY

In Sec. IV, we showed that predissociation lifetimes increase with decreasing binding energy of the complex. Therefore, the lifetime of the most weakly bound complex will control the relaxation for high atom densities. This lifetime may be estimated using the effective range formula [9]

$$\tau_{vj}^{-1} = \frac{2\beta_{vj}}{\mu r_{vj} |a_{vj}|^2} \left\{ \left[1 - \frac{2\alpha_{vj} r_{vj}}{|a_{vj}|^2} \right]^{-1/2} - 1 \right\}, \quad (44)$$

where $a_{vj} = \alpha_{vj} - i\beta_{vj}$ is the complex scattering length and r_{vj} is the effective range. We follow the notational convention that the label n will be suppressed when referring to the most weakly bound level of the van der Waals complex. It has been shown [8,9] that the imaginary part of the scattering length is given by

$$\beta_{vj} = \frac{\mu}{4\pi} \lim_{T \rightarrow 0} R_{vj}(T). \quad (45)$$

Recalling the kinetic model of Sec. II, we conclude that when the density of atoms in the trap is large, the system relaxes primarily through the process of vibrational predissociation. This relaxation process is independent of temperature. However, using Eqs. (44) and (45) we see that a measurement of the vibrational relaxation performed at high temperature and high density would yield information about the total collisional quenching rate also at zero temperature. This piece of information is extremely valuable in determining whether a trapped molecular species could be efficiently cooled to ultracold temperatures.

If the effective range is small, the scattering length approximation may be used to obtain

$$\lim_{T \rightarrow 0} \frac{\tau_{vj}^{-1}}{R_{vj}(T)} = \frac{1}{2\pi\alpha_{vj}^3} = \frac{(2\mu I)^{3/2}}{2\pi}. \quad (46)$$

The relationship between rate coefficient and predissociation lifetime given in Eq. (46) may be understood from a simple physical picture. The typical spread L of the wave function for a weakly bound state depends on the binding energy: $L = 1/\sqrt{2\mu I}$. The effective density of atoms in the active area

is estimated as $[A] \sim 1/L^3$. The decay rate of predissociation may then be calculated as $\tau_{vj}^{-1} = \lim_{T \rightarrow 0} R_{vj}(T)[A]$ in accordance with Eq. (46).

VI. COMPLEX FORMATION AND DECAY

In order to complete our analysis of the kinetic model presented in Sec. II, we need to determine the forward and backward rate coefficients k_f and k_b . In general, these parameters are extremely difficult to compute, and are beyond the scope of this work. However, we may use detailed balance to remove the backward rate coefficient k_b from the analysis. At low temperatures, the forward rate coefficient k_f is independent of temperature due to Wigner's threshold law for inelastic collisions. Therefore, in the following discussion, we ignore the temperature dependence of k_f . If we restrict the complex formation and decay process (2) to include only s waves, then

$$k_b(T) = k_f[A] \exp(-I/k_B T). \quad (47)$$

The temperature dependence of the relaxation parameter γ defined in Eq. (16) is then given by

$$\frac{\gamma(T)}{[A]} = \frac{R_{vj}(T) + k_f[A]}{\tau_{vj}^{-1} + k_f[A]^2 \exp(-I/k_B T)}. \quad (48)$$

When $I \ll k_B T$,

$$\gamma(T) = \begin{cases} \tau_{vj} R_{vj}(T)[A], & [A] \rightarrow 0, \\ \exp(I/k_B T), & [A] \rightarrow \infty. \end{cases} \quad (49)$$

When $I \gg k_B T$,

$$\gamma(T) = \begin{cases} 2\pi\alpha_{vj}^3[A], & [A] \rightarrow 0, \\ \tau_{vj} k_f [A]^2, & [A] \rightarrow \infty. \end{cases} \quad (50)$$

At low temperatures, the predissociation relaxation path is important when the density satisfies the condition $[A] \gg (\tau_{vj} k_f)^{-1/2}$. In the zero-temperature limit, the backward rate coefficient k_b approaches zero exponentially fast and the predissociation relaxation path becomes negligible.

VII. RESULTS

The kinetic model is tested for the two isotopes of helium interacting with vibrationally excited H_2 . The parameters are obtained from full quantum-mechanical calculations on a reliable potential energy surface: the HeH_2 interaction potential of Muchnick and Russek [14] and the H_2 potential of Schwenke [15]. We find that the weakly bound $He \cdots H_2$ complex supports one bound state for each of its associated diatomic vibrational levels. Figure 1 shows the channel potential and the bound state wave functions for the $v=0, j=0$ complex of ${}^3He \cdots H_2$ and ${}^4He \cdots H_2$. Both wave functions are very diffuse, extending to distances of 100 Å and beyond. The binding energy of the ${}^3He \cdots H_2$ complex is 0.0016 cm^{-1} whereas for ${}^4He \cdots H_2$ it is 0.0298 cm^{-1} . This difference in binding energy is responsible for the large difference in the elastic scattering cross sections for 3He and 4He collisions with H_2 shown in Fig. 2. The inelastic scat-

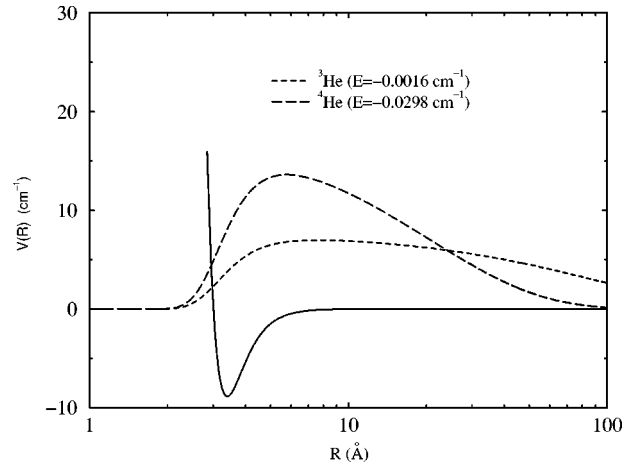


FIG. 1. Channel potential (solid curve) and bound state wave functions for the $v=0, j=0$ complex of ${}^3He \cdots H_2$ and ${}^4He \cdots H_2$.

tering cross sections for 3He and 4He collisions with H_2 are shown in Fig. 3. The difference between the two cross sections in Fig. 3 is due to the differences in the two binding energies of the $He \cdots H_2$ complexes for $v=1$.

Figure 4 shows the relaxation of $[H_2(v=1, j=0)]_t$ due to interaction with 4He atoms at a temperature of 10 mK. For the calculation, we used the predissociation lifetime and binding energy given by Forrey *et al.* [9] of 0.069 sec and 0.0282 cm^{-1} , respectively. We assumed $\gamma = 6.9$ which is equivalent to $k_f[A]^2 = 100$. It is clear from Fig. 4 that a measurement of vibrational relaxation with time in the $\gamma \gg 1$ case would provide valuable information. The short time scale would give the forward rate coefficient k_f and the long time scale the predissociation lifetime τ_{vj} . The binding energy of the van der Waals complex could be obtained from the measurement using the formula

$$I = -k_B T \ln(c_2/\gamma), \quad (51)$$

where c_2 is the y intercept of the coefficient predissociation curve. The zero-temperature quenching rate could then be determined from τ_{vj} and I using Eq. (46).

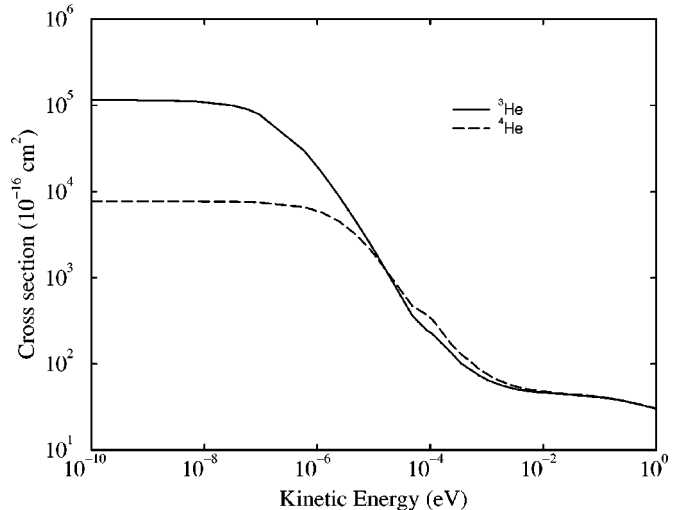


FIG. 2. Elastic scattering cross section for 3He and 4He collisions with $H_2(v=0, j=0)$.

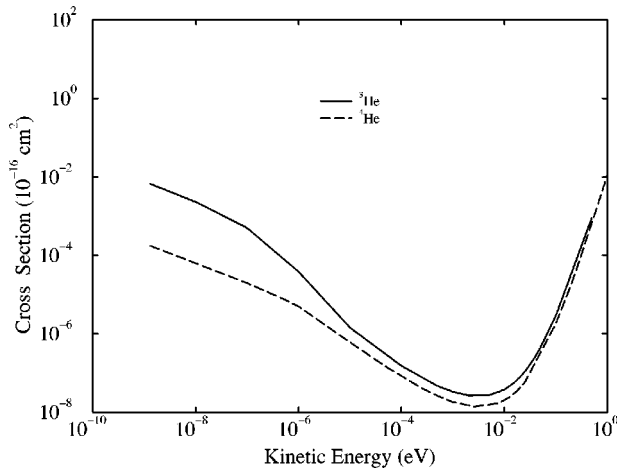


FIG. 3. Inelastic scattering cross section for ^3He and ^4He collisions with $\text{H}_2(v=1, j=0)$.

The discussion given above may be generalized to systems possessing more than one bound level of the van der Waals complex. Figure 5 shows how the high density relaxation plot would look for a system that supports two bound levels. As before, the short time scale would be given by the collisional process. The intermediate time scale would be given by the predissociation lifetime corresponding to the most deeply bound state, and the long time scale would be given by the predissociation lifetime of the loosely bound complex.

VIII. DISCUSSION

Effective range theory is often used to show that the position of the last bound state for a radially symmetric potential has a strong influence on the elastic scattering cross section as the collision energy is reduced to zero. In the present work, we have extended the theory to include potentials that are not radially symmetric. It is shown that the position of the last bound state has a strong influence on both the elastic and the inelastic scattering cross sections when the collision energy is small.

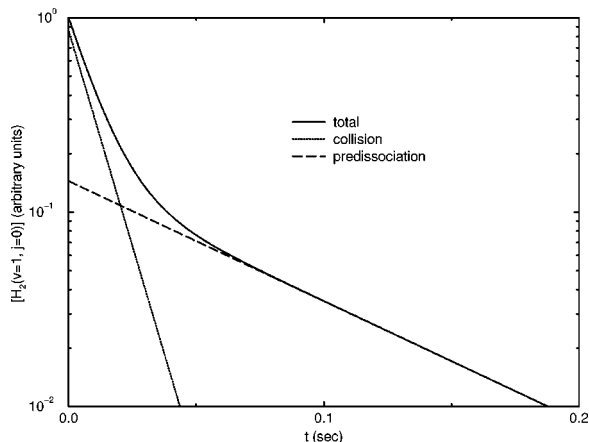


FIG. 4. Vibrational relaxation of trapped $\text{H}_2(v=1, j=0)$ due to interaction with ^4He at 10 mK. The dotted curve is the time scale due to collisions, and the dashed curve is the time scale due to predissociation. The solid curve is the total relaxation time.

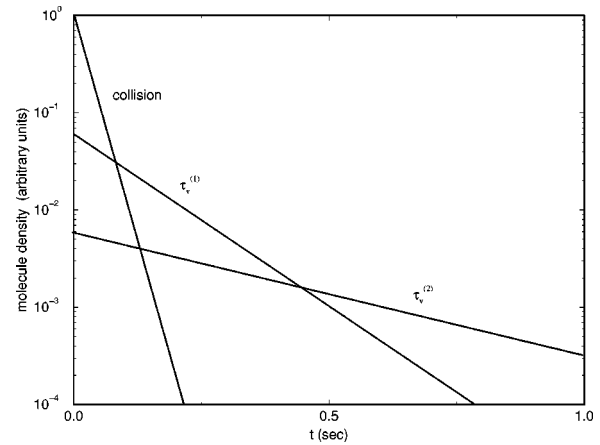


FIG. 5. Simulated relaxation for a system possessing two quasibound levels. At high atom density, the relaxation is controlled by the quasibound level with the longest lifetime.

Using a simple kinetic model, we have shown that if the density of atoms in a trap is large, vibrationally excited molecules relax primarily through the process of vibrational predissociation. The rate of predissociation of the weakly bound complex decreases with the binding energy of the complex so that the predissociating state with the smallest binding energy controls the relaxation rate at high densities. At low atom densities, the relaxation is determined primarily by the direct collisional quenching process. Therefore, the most weakly bound state of the van der Waals complex actually controls the relaxation for all atom densities.

Measurement of relaxation in the high density case would provide direct information about the rate coefficients $k_{f,n}$ and $k_{b,n}$ as well as the predissociation lifetimes $\tau_{vj,n}$ and binding energies $I_{vj,n}$ of the complex and the zero-temperature quenching rate coefficients R_{vj} . We argue that the use of trapped molecules to measure Feshbach resonance parameters would provide a stringent test of atom-molecule potential energy surfaces [9]. The high density limit of the kinetic model described in the present work may provide a useful experimental method for obtaining such information.

ACKNOWLEDGMENT

The work of R.C.F. was supported by the U.S. Department of Energy, Office of Basic Energy Sciences, Office of Energy Research.

APPENDIX: MORSE POTENTIAL

To illustrate the general formulas derived in Sec. III, we analyze the physical properties of weakly bound states for an exactly solvable problem. If the interaction in the initial state can be described by the Morse potential

$$V_{ii}(R) = V_0(e^{-2(R-R_c)/a} - 2e^{-(R-R_c)/a}), \quad (\text{A1})$$

then the energy and wave function of the weakly bound state will depend on the potential strength $\xi = 2mV_0a^2$ as follows:

$$I = V_0 \left(1 - \frac{1}{2\sqrt{\xi}} \right)^2 \quad (\text{A2})$$

and

$$\chi_i(R) = \sqrt{\frac{1}{a\Gamma(2\kappa a)}} (2\sqrt{\xi} e^{-(R-R_c)/a})^{\kappa a} \times \exp[-\sqrt{\xi} e^{-(R-R_c)/a}]. \quad (\text{A3})$$

The condition of a weakly bound state is satisfied if the potential strength can be expressed as $\xi = 1/4 + \beta$, where $\beta \ll 1$. Asymptotic expressions for the binding energy and the wave function of weakly bound states are then given by

$$I \approx 4\beta^2 V_0, \quad \beta \ll 1, \quad (\text{A4})$$

$$\chi_i(R) \approx \sqrt{2\kappa} e^{-\kappa(R-R_c)} \exp\left[-\frac{1}{2} e^{-(R-R_c)/a}\right]. \quad (\text{A5})$$

Asymptotic solutions for the Morse potential can be compared with the general asymptotic solutions given in Sec. III. The normalization factor $N_{\text{Morse}} = \sqrt{2\kappa}$ given in Eq. (A5) is equal to the normalization constant for the general case given by Eq. (42). The wave function of the weakly bound state for the Morse potential in the external area $R > R_0$ is described by the same asymptotics as Eq. (37),

$$\chi_i(R) \approx \chi_{>}(R) = \sqrt{2\kappa} e^{-\kappa R}, \quad R > R_0 = R_c + \eta a, \quad (\text{A6})$$

where η is an arbitrary number of units. For simplification we assume that the radius R_c of the equilibrium position is comparable with the width a of the Morse potential well, i.e., $\kappa a \sim \kappa R_c \ll 1$. Internal solution in the active area $R \sim R_c \pm \eta a$ depends on the binding energy from the normalization factor $N(I)$ only,

$$\chi_i(R) \approx \chi_{<}(R) = \sqrt{2\kappa} \exp\left[-\frac{1}{2} e^{-(R-R_c)/a}\right], \quad (\text{A7})$$

as shown in Sec. III. The radial part of the internal solution $\psi_0(R)$ corresponds with exponential accuracy to the solution with zero energy boundary conditions at $R_0 = R_c + \eta a$ given by

$$\psi_0(R=R_0) = \exp\left[-\frac{1}{2} e^{-\eta}\right] \approx 1 \quad (e^{-\eta} \ll 1), \quad (\text{A8})$$

$$\left. \frac{d\psi_0(R)}{dR} \right|_{R=R_0} = -\frac{e^{-\eta}}{2a} \psi_0(R=R_0) \approx 0. \quad (\text{A9})$$

Matrix elements of predissociative decay for different channels will depend on the binding energy only via the normalization factor $N(I)$, and the total predissociation rate Γ_i will include $N(I)$ as the only dependence on the binding energy.

-
- [1] J. M. Doyle, B. Friedrich, J. Kim, and D. Patterson, *Phys. Rev. A* **52**, R2515 (1995).
- [2] J. T. Bahns, W. C. Stwalley, and P. L. Gould, *J. Chem. Phys.* **104**, 9689 (1996).
- [3] A. Fioretti, D. Comparat, A. Crubellier, O. Dulieu, F. Masnou-Seeuws, and P. Pillet, *Phys. Rev. Lett.* **80**, 4402 (1998).
- [4] T. Takekoshi, B. M. Patterson, and R. J. Knize, *Phys. Rev. A* **59**, R5 (1999).
- [5] J. D. Weinstein, R. deCarvalho, T. Guillet, B. Friedrich, and J. M. Doyle, *Nature (London)* **395**, 148 (1998).
- [6] N. Balakrishnan, R. C. Forrey, and A. Dalgarno, *Chem. Phys. Lett.* **280**, 1 (1997).
- [7] N. Balakrishnan, R. C. Forrey, and A. Dalgarno, *Phys. Rev. Lett.* **80**, 3224 (1998).
- [8] N. Balakrishnan, V. Kharchenko, R. C. Forrey, and A. Dalgarno, *Chem. Phys. Lett.* **280**, 5 (1997).
- [9] R. C. Forrey, N. Balakrishnan, V. Kharchenko, and A. Dalgarno, *Phys. Rev. A* **58**, R2645 (1998).
- [10] G. Ewing, *Chem. Phys.* **29**, 253 (1978).
- [11] J. M. Hutson and S. Green, MOLSCAT computer code, version 14 (1994), distributed by Collaborative Computational Project No. 6 of the Engineering and Physical Sciences Research Council (U.K.).
- [12] A. M. Arthurs and A. Dalgarno, *Proc. R. Soc. London, Ser. A* **A256**, 540 (1963).
- [13] J. M. Hutson, C. J. Ashton, and R. J. LeRoy, *J. Phys. Chem.* **87**, 2713 (1983).
- [14] P. Muchnick and A. Russek, *J. Chem. Phys.* **100**, 4336 (1994).
- [15] D. W. Schwenke, *J. Chem. Phys.* **89**, 2076 (1988).